First principles study of oxygen vacancy defects in tantalum pentoxide

R. Ramprasad[a)]
Semiconductor Products Sector, Motorola, Inc., 2100 East Elliot Road, Tempe, Arizona 85284

(Received 14 April 2003; accepted 11 August 2003)

First principles total energy calculations were performed to characterize oxygen vacancy defects in tantalum pentoxide (Ta_2O_5). A simplified version of the crystalline orthorhombic phase of Ta_2O_5 was used in this study. Results indicate that O vacancies in Ta_2O_5 can be broadly classified based on their location in the lattice. One type of vacancy that occupies the ''in-plane'' sites displays deep or midgap occupied states and shallow unoccupied states, while a second type occupying ''cap'' sites results in shallow occupied states. For a wide range of Fermi levels or chemical potentials, the neutral and +2 charged states of the in-plane type vacancy and the +2 charge state of the cap type vacancy are found to be most stable. © *2003 American Institute of Physics.*
[DOI: 10.1063/1.1615700]

I. INTRODUCTION

Although tantalum pentoxide (Ta_2O_5) has been studied both experimentally and theoretically over the past three decades, its real emergence as a dielectric material that can be integrated with conventional complementary metal–oxide–semiconductor processes has happened only in the last decade.[1–4] While interest in high dielectric constant materials is primarily due to a need to scale down device sizes, the renewed interest in Ta_2O_5 is also due to the ability to deposit it using conventional methods compatible with equipment and processes already available in the semiconductor industry. Nevertheless, concerns exist with Ta_2O_5 and other alternative dielectric materials, one of them being defect densities and their impact on the leakage currents via defect or ''trap'' levels created in the band gap of the dielectric.

The present work attempts to theoretically characterize oxygen vacancy defects in Ta_2O_5. Oxygen vacancies are expected to be the most predominant type of defect in metal–oxide dielectrics. The atomistic structure of Ta_2O_5 was chosen so that it is computationally tractable, while at the same time is representative of deposited films. Different types of O vacancies with qualitatively different types of coordination environments were considered within this model, and the defect or trap levels due to these defects were determined using first principles total energy calculations. Correlations between the coordination environment of the oxygen vacancy defects and the location of the defect levels were identified. The stability of variously charged vacancies was also considered, as a function of the vacancy type and the local chemical potential.

This article is organized as follows. In the next section, we provide details of the calculation methods and the atomistic model of Ta_2O_5 used in this work. Section III discusses the results: structural aspects of the local coordination environment of Ta ions in Ta_2O_5 are compared with measurements in Sec. III A, the location of O vacancy induced defect levels in the band gap of Ta_2O_5 is discussed in Sec. III B, and the relative stability of charged O vacancies is presented in Sec. III C. We finally conclude with Sec. IV.

II. MODEL AND METHOD

Crystalline Ta_2O_5 occurs in several different polymorphs, with the orthorhombic phase, containing 11 formula units (22 Ta and 55 O atoms) being the most stable.[5] The building blocks of the orthorhombic structure are octahedral TaO_6 and pentagonal bipyramidal TaO_7 polyhedra.[5] While as-deposited Ta_2O_5 is either amorphous or polycrystalline,[6] the basic building blocks still appear to be TaO_6 and TaO_7 polyhedra.[6] This is similar to SiO_2, where the basic building blocks are SiO_4 tetrahedra, irrespective of whether the structure is amorphous or crystalline. In the present work, for computational ease, a simplified version of the actual orthorhombic unit cell containing two Ta_2O_5 formula units (4 Ta and 10 O atoms) consisting of two TaO_6 and two TaO_7 polyhedra was used (Fig. 1). Although our chosen model of Ta_2O_5 is crystalline, it will be shown in the next section that the local environment of Ta and O is consistent with that of fabricated Ta_2O_5 films. Since it is the immediate local environment of Ta and O (rather than the large scale symmetry of the structure) that determines the properties of interest to us, we believe that our model constitutes a reasonable approximation. Prior density functional studies of Ta_2O_5 include an oxygen vacancy study by Sawada and Kawakami[7] and a defect free hexagonal Ta_2O_5 study by Fukumoto and Miwa.[8] Like the present investigation, the former study[7] also involved a (different) simplified version of the orthorhombic Ta_2O_5 structure. However, we found that our Ta_2O_5 model had lower total energy per formula unit than that of either Sawada and Kawakami or Fukumoto and Miwa.

All results reported here were obtained from calculations performed using the local density approximation (LDA) within the density functional theory, as implemented in the Vienna *ab initio* simulation package (VASP).[9] Ultrasoft pseudopotentials were used to represent the Ta and O atoms in the $6s^15d^4$ and $2s^22p^4$ valence electronic configurations, respectively. A plane-wave basis set with an energy cutoff of

a)Electronic mail: r.ramprasad@motorola.com

 © 2003 American Institute of Physics

Downloaded 13 Sep 2006 to 137.99.20.141. Redistribution subject to AIP license or copyright, see http://jap.aip.org/jap/copyright.jsp

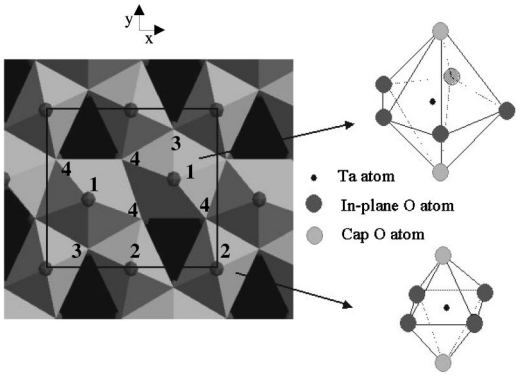

FIG. 1. Schematic of the Ta_2O_5 structure used in the present calculation, with the rectangle highlighting the unit cell. Also shown are perspective views of the TaO_7 (top, right) and TaO_6 (bottom, right) building blocks, with the in-plane and cap site O locations explicitly identified. The four symmetry-inequivalent atoms are labeled within the unit cell, with labels 1 and 2 denoting cap sites and labels 3 and 4 denoting in-plane sites. Oxygen vacancy calculations were performed with twice the size of the bulk unit cell, with the two unit cells stacked along the *z* axis.

29 Ry for the wave function and 68 Ry for the electron density was used. Defect free bulk Ta_2O_5 calculations were performed with 12 k points in the irreducible wedge of the Brillouin zone (IBZ); increasing the number of k points was found to have negligible effects on both the structure and the total energy. The structure used for the oxygen vacancy calculations was twice the size of the bulk unit cell and contained 8 Ta and 19 O atoms; 8 k points were used in the IBZ. Further doubling the size of the unit cell for the O vacancy calculation had negligible effects on the vacancy formation energy. All calculations involved relaxation of the atomic positions until the forces on each atom were below 0.04 eV/A. A limited number of initial calculations were performed using the generalized gradient approximation (GGA); the relative energy trends for defect structures were identical to that obtained using the LDA method. Owing to this consistency, and the facts that the GGA does not provide a systematic correction to the LDA results for band energies, that the deficiencies of the LDA are better understood, and that we are primarily interested in general trends in this work, all subsequent calculations were performed using the LDA.

The Ta_2O_5 band gap and energies of oxygen vacancy induced defect states in the band gap were calculated using total energy results of separate neutral, $+1$ and -1 charged calculations as described earlier.[10] The band gap (E_{gap}) was determined as

$$E_{\text{gap}} = E(\text{per},-1) + E(\text{per},+1) - 2E(\text{per},0), \tag{1}$$

where $E(\text{per},q)$ is the total energy per supercell of the defect-free structure with charge q.[11] The calculated band gap using the above formula for Ta_2O_5 was 2.43 eV, while the experimental value is 4.0 eV.[4] Sawada and Kawakami[7] calculate a value of 2.3 eV for the band gap. Such a discrepancy between calculated and measured values is to be expected when the LDA is used. All energies in the band gap were then scaled by κ, the ratio of the experimental to the theoretical values of the band gap ($\kappa = 1.65$ in our case). The states in the band gap created due to oxygen vacancies are determined from the ionization potential (IP) and the electron affinities (EA) determined relative to the valence band maximum as

$$\text{IP} = \kappa \cdot [E(\text{per},+1) - E(D,+1) - E(\text{per},0) + E(D,0)], \tag{2}$$

$$\text{EA} = \kappa \cdot [E(\text{per},+1) - E(D,0) - E(\text{per},0) + E(D,-1)], \tag{3}$$

where $E(D,q)$ is the total energy per supercell with charge q containing an oxygen vacancy.[11] The above procedure is identical to the one adopted by Foster *et al.*[10] except that we scale our defect energies by κ rather than rigidly shift the bottom of the conduction band by the difference between the experimental and theoretical band gaps. While both scaling procedures are *ad hoc*, we believe that ours is more realistic; by construction, the approach of Foster *et al.* is incapable of resulting in defect levels close to the conduction band minimum by less than the difference between the experimental and theoretical band gaps.

The stability of charged systems relative to their neutral counterparts is determined by evaluating the difference between $E(D,q) + \mu q$ and $E(D,0)$, where μ is the electronic chemical potential.[12] The electronic chemical potential close to, say, a metal–dielectric interface is determined by the Fermi level (E_F) of the metal. The relative total energy of the charged vacancy supercell with respect to the corresponding neutral system is thus given as $E(D,q) + qE_F - E(D,0)$. Since it is convenient to reference E_F to the valence band maximum (E_V) of the dielectric, the relative total energy after correcting for the LDA underestimation of the band gap is given by

$$E^{\text{rel}}(D,q) = E(D,q) + qE_V - E(D,0) + q(E_F - E_V)/\kappa \tag{4}$$

$$= E(D,q) + q[E(\text{per},0) - E(\text{per},+1)] - E(D,0) + q(E_F - E_V)/\kappa. \tag{5}$$

$E^{\text{rel}}(D,q)$ is typically plotted as a function of $(E_F - E_V)$ for various charge states, and all other quantities appearing in the earlier equation are determined from charged and neutral supercell calculations.

III. RESULTS AND DISCUSSION

A. Local environment of Ta ions in Ta_2O_5

The optimal orthorhombic unit cell dimensions for our defect free Ta_2O_5 model system was determined to be 7.13, 6.03, and 3.82 Å along the *x*, *y*, and *z* axes (according to the axes definition of Fig. 1). The optimized coordinates of all 14 atoms in the unit cell are listed in Table I. The nearest neighbor Ta–O bond lengths for the TaO_6 and TaO_7 polyhedra calculated here are in the 1.98–2.00 and 1.92–2.56 Å ranges, respectively, in good agreement with those observed for the actual orthorhombic crystal structure.[5] More significantly, the nearest neighbor Ta–O distances observed in amorphous Ta_2O_5 films formed under typical deposition conditions is 2.05–2.06 Å, and the average coordination number (defined as the number of O atoms directly bonded to a Ta atom) of

Downloaded 13 Sep 2006 to 137.99.20.141. Redistribution subject to AIP license or copyright, see http://jap.aip.org/jap/copyright.jsp

TABLE I. Atomic coordinates, in lattice units, of all 14 atoms in the defect-free Ta_2O_5 unit cell as per the axes definition of Fig. 1.

Atom type	*x* coordinate	*y* coordinate	*z* coordinate
Ta	0.000	0.000	0.000
Ta	0.500	0.000	0.000
Ta	0.250	0.456	0.000
Ta	0.750	0.539	0.000
O	0.000	0.991	0.500
O	0.500	0.991	0.500
O	0.250	0.429	0.500
O	0.750	0.556	0.500
O	0.059	0.679	0.000
O	0.251	0.117	0.000
O	0.564	0.308	0.000
O	0.444	0.679	0.000
O	0.751	0.872	0.000
O	0.939	0.308	0.000

such films turns out to be 6.1–7.8.[6] Thus, the local coordination environment of Ta in the present model is consistent with that for amorphous Ta_2O_5 films, justifying the present approach for calculating properties that are largely determined by the local bonding environment.

B. O vacancy induced defect states

We next focus on the energetic location of defect levels created due to O vacancies. Based on the local environment, we classify O atomic and vacancy sites into the two types shown in Fig. 1: ''in-plane'' sites that form the base of the pentagon or the quadrilateral of the polyhedra, and ''cap'' sites that cap the basal planes of the polyhedra. For the chosen model of Ta_2O_5, two distinct symmetry-inequivalent cap sites (labeled as 1 and 2 in Fig. 1) and two distinct in-plane sites (labeled as 3 and 4) are present. As we will see, the cap and in-plane types of vacancies display qualitatively different behavior. Lattice relaxations due to creation of in-plane type vacancies are expected to occur more easily than those due to cap type vacancies, as the in-plane O atoms are shared by three polyhedra, while the cap O atoms are shared only by 2.

Creation of a neutral O vacancy in metal oxides leaves behind two electrons localized close to the vacancy location. In Ta_2O_5, as in many other oxides,[10,13] these electrons occupy the lower of two energy states created at the band gap (the bonding orbital), with the upper state (the antibonding orbital) completely empty. Thus, the occupied and the unoccupied state energies are essentially the IP and EA, respectively, defined in the previous section and are displayed in Fig. 2 for the two distinct in-plane and the two distinct cap site vacancies both before and after relaxation of the lattice. Also shown at the bottom of the plot are the relaxed vacancy formation energies calculated relative to an isolated oxygen atom, and the site labels indicating the location of each vacancy.

The following observations can be made: (i) in-plane type vacancies result in occupied levels at the midgap energy range and shallow unoccupied levels; (ii) cap type vacancies display shallow occupied states and the unoccupied states buried in the conduction band; (iii) lattice relaxations can cause shifts of up to 0.6 eV, specially in the case of occupied levels; and (iv) the vacancy formation energies (shown at the bottom of Fig. 2) of in-plane vacancies are in general lower than those of cap vacancies. Observations (i) and (ii) are consistent with photoemission measurements made by Fleming *et al.*,[4] where features in the emission spectra due to midgap and shallow states can be clearly seen. Sawada and Kawakami[7] consider only one O vacancy in their work. Although they do not state it explicitly, it is clear from their Fig. 6 that their's is an in-plane type vacancy which displays an occupied state 0.8 eV below the conduction band minimum. After correcting for the LDA band gap underestimation, this value increases to about 1.4 eV, consistent with our result for the in-plane type vacancy with site label 4.

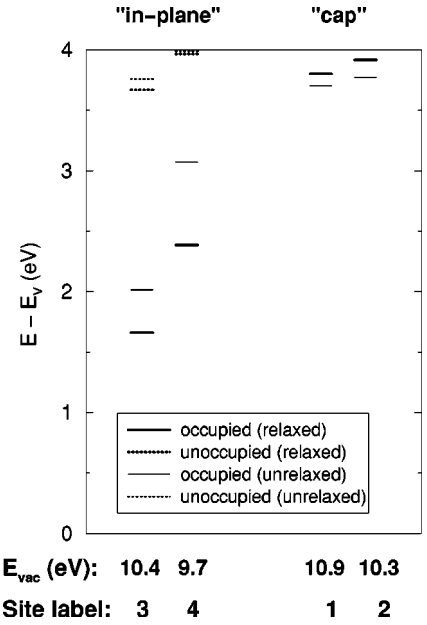

FIG. 2. Occupied and unoccupied in-plane and cap site O vacancy induced defect states, before and after lattice relaxation. Results for two vacancies of each type are shown. One of the in-plane vacancies (site label 3) is shared by 2 TaO_6 and 1 TaO_7 polyhedra, where as the second in-plane vacancy (site label 4) is shared by 1 TaO_6 and 2 TaO_7 polyhedra. One of the cap site vacancies (site label 1) is shared by 2 TaO_7 polyhedra where as the other (site label 2) is shared by 2 TaO_6 polyhedra. Vacancy formation energies calculated relative to an isolated oxygen atom, and the site labels indicating the location of each vacancy, are listed below the energy level diagram. All defect state energies are referenced to the top of the valence band, and shifted to reflect the experimental band gap of 4.0 eV.

C. Relative stability of charged vacancies

The stability of a charge state of a vacancy is determined by the position of the vacancy induced defect levels with respect to the local chemical potential. For vacancies close to the metal–insulator interface, the local chemical potential is largely determined by the metal Fermi level. Figure 3 displays the relative total energies of one of the in-plane (site label 4) and one of the cap (site label 1) vacancies in different charge states as a function of the local chemical potential or Fermi energy, relative to the valence band minimum of Ta_2O_5. The lattice structure for each charge state was completely relaxed. In each case, the total energy is referenced to that of the neutral vacancy.

Downloaded 13 Sep 2006 to 137.99.20.141. Redistribution subject to AIP license or copyright, see http://jap.aip.org/jap/copyright.jsp

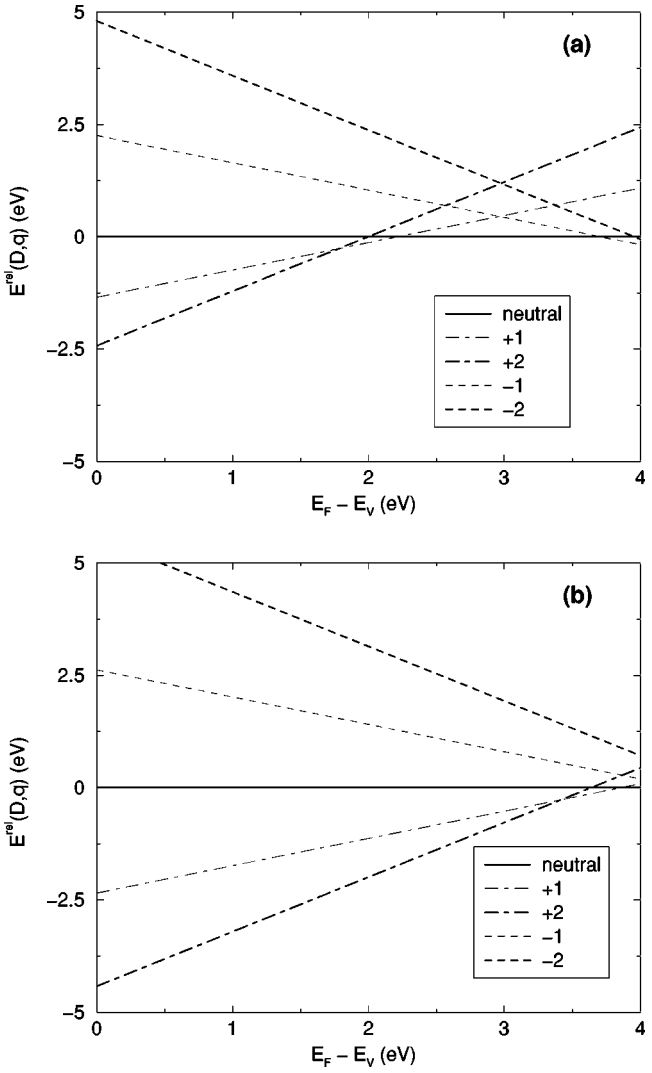

FIG. 3. Relative total energy $E^{\mathrm{rel}}(D,q)$ of (a) the in-plane vacancy with site label 4 and (b) the cap type vacancy with site label 1, as a function of the local Fermi energy, where q denotes the charge state of the vacancy ($q=+2$, $+1$, 0, -1, or -2).

Consider Fig. 3(a). For very low values of the local Fermi energy, the $+2$ charged state of the vacancy is predicted to be most stable, and for medium to high values of E_F-E_V, the neutral state is seen to be most stable. These predictions are consistent with the location of the occupied state at the mid gap energy range, and the unoccupied state close to the conduction band maximum in the case of in-plane type vacancies. Clearly, when E_F-E_V is very low, the two electrons from the occupied state will tend to be transferred to the Fermi level, making the $+2$ state more stable, while no transfer of charge will occur for most other values of E_F-E_V, making the neutral state most stable. Thus, with the exception of the small E_F-E_V ranges at which the $+1$ and -1 charge states are stable, the $+2$ and neutral states are seen to be the most stable for a wide range of E_F-E_V. Similar arguments hold for the cap site vacancy [Fig. 3(b)], for which the $+2$ charged state is most stable for a wide range of Fermi energies.

IV. SUMMARY

Density functional calculations were performed in order to characterize O vacancy defects in Ta_2O_5. A simplified version of the crystalline orthorhombic phase of Ta_2O_5 was used in this study. The local coordination environment of the present model was found to be similar to that of Ta_2O_5 films. Results indicate that O vacancies in Ta_2O_5 can be broadly classified into in-plane and cap types, based on their location in the lattice. The in-plane vacancies display deep or mid gap level occupied states and shallow unoccupied states, while the cap vacancies produce shallow occupied states. For a wide range of possible Fermi level positions, the neutral and $+2$ charged states of the in-plane type vacancy and the $+2$ charge state of the cap type vacancy are most stable.

ACKNOWLEDGMENTS

The author would like to acknowledge Leonardo Fonseca for help with the VASP code, and several stimulating discussions with Tom Remmel and Mike Petras. Mike Petras and Mel Miller are also acknowledged for critically reading the manuscript.

[1] C. Chaneliere, J. L. Autran, R. A. B. Devine, and B. Balland, Mater. Sci. Eng., R. **22**, 269 (1998).
[2] C. C. Barron *et al.*, Proceedings of the 202nd Electrochemical Society, October, 2002.
[3] D. R. Roberts, S. Kalpat, T. P. Remmel, M. A. Sadd, M. V. Raymond, R. Ramprasad, E. D. Luckowski, and M. Miller, Proceedings of the 202nd Electrochemical Society, October, 2002.
[4] R. M. Fleming *et al.*, J. Appl. Phys. **88**, 850 (2000).
[5] N. C. Stephenson and R. S. Roth, Acta Crystallogr., Sect. B: Struct. Crystallogr. Cryst. Chem. **B27**, 1037 (1971).
[6] H. Kimura, J. Mizuki, S. Kamiyama, and H. Suzuki, Appl. Phys. Lett. **66**, 2209 (1995).
[7] H. Sawada and K. Kawakami, J. Appl. Phys. **86**, 956 (1999).
[8] A. Fukumoto and K. Miwa, Phys. Rev. B **55**, 11155 (1997).
[9] G. Kresse and J. Hafner, Phys. Rev. B **47**, 558 (1993); G. Kresse and J. Furthmuller, *ibid.* **54**, 11169 (1996).
[10] A. S. Foster, V. B. Sulimov, F. Lopez Gejo, A. L. Shluger, and R. M. Nieminen, Phys. Rev. B **64**, 224108 (2001).
[11] Charged calculations were performed using the standard technique of imposing a charge neutralizing homogeneous background charge and correcting for spurious dipole interactions. For instance, see http://cms.mpi.univie.ac.at/vasp/vasp/vasp.html, and G. Makov and M. C. Payne, Phys. Rev. B **51**, 4014 (1995).
[12] A. Yokozawa and Y. Miyamoto, Phys. Rev. B **55**, 13783 (1997); A. Garcia and J. E. Northrup, Phys. Rev. Lett. **74**, 1131 (1995).
[13] A. S. Foster, F. Lopez Gejo, A. L. Shluger, and R. M. Nieminen, Phys. Rev. B **65**, 174117 (2002).

Downloaded 13 Sep 2006 to 137.99.20.141. Redistribution subject to AIP license or copyright, see http://jap.aip.org/jap/copyright.jsp